



HAL
open science

Quantitative dual isotope ^{123}I / $^{99\text{m}}\text{Tc}$ -MIBI scintigraphy: A new approach to rule out malignancy in thyroid nodules

Hamza Benderradji, Amandine Beron, Jean-Louis Wémeau, Bruno Carnaille, Laurent Delcroix, Christine Do Cao, Clio Baillet, Damien Huglo, Georges Lion, Samuel Boury, et al.

► To cite this version:

Hamza Benderradji, Amandine Beron, Jean-Louis Wémeau, Bruno Carnaille, Laurent Delcroix, et al.. Quantitative dual isotope ^{123}I / $^{99\text{m}}\text{Tc}$ -MIBI scintigraphy: A new approach to rule out malignancy in thyroid nodules. *Annales d'Endocrinologie = Annals of Endocrinology*, 2021, 82 (2), pp.83-91. 10.1016/j.ando.2021.03.003 . hal-04525532

HAL Id: hal-04525532

<https://hal.science/hal-04525532v1>

Submitted on 22 Jul 2024

HAL is a multi-disciplinary open access archive for the deposit and dissemination of scientific research documents, whether they are published or not. The documents may come from teaching and research institutions in France or abroad, or from public or private research centers.

L'archive ouverte pluridisciplinaire **HAL**, est destinée au dépôt et à la diffusion de documents scientifiques de niveau recherche, publiés ou non, émanant des établissements d'enseignement et de recherche français ou étrangers, des laboratoires publics ou privés.



Distributed under a Creative Commons Attribution - NonCommercial 4.0 International License

Quantitative dual isotope ^{123}I iodine/ $^{99\text{m}}\text{Tc}$ -MIBI scintigraphy: a new approach to rule out malignancy in thyroid nodules
Scintigraphie au $^{99\text{m}}\text{Tc}$ -MIBI combinée à l'iode 123 : une nouvelle approche pour l'exclusion de malignité des nodules thyroïdiens

Authors:

Hamza Benderradji ^{1,2}, Amandine Beron ³, Jean-Louis Wémeau ¹, Bruno Carnaille ⁴, Laurent Delcroix³, Christine Do Cao ¹, Clio Baillet ³, Damien Huglo ^{3,5}, Georges Lion ³, Samuel Boury ⁶, Jean-Félix Cussac ⁶, Robert Caiazza ^{4,7}, François Pattou ^{4,7}, Emmanuelle Leteurtre ^{8,9}, Marie-Christine Vantighem ^{1,7}, Miriam Ladsous ^{1,10}

(1) Department of Endocrinology, Diabetology, and Metabolism, Lille University Hospital, Lille, France.

(2) Lille University, Inserm, U 1172, Lille, France.

(3) Department of Nuclear Medicine, Lille University Hospital, Lille, France.

(4) Department of General and Endocrine Surgery, Lille University Hospital, Lille, France.

(5) Lille University, Inserm, U 1189, Lille, France.

(6) Department of Radiology, Lille University Hospital, Lille, France.

(7) Lille University, Inserm, U1190-EGID, Lille, France.

(8) Department of Pathology, Lille University Hospital, Lille, France.

(9) Lille University, CNRS, UMR9020, Inserm, U1277 - CANTHER - Cancer Heterogeneity, Plasticity and Resistance to Therapies, Lille, France.

(10) Department of Endocrinology, Valenciennes General Hospital, France

Corresponding author:

Dr. Hamza Benderradji

Department of Endocrinology, Diabetology and Metabolism

Lille University Hospital

1 Place de Verdun 59045 Lille Cedex, France

hamza.benderradji@inserm.fr

+33 (0)6 13 18 50 31

1 **Abstract**

2 **Background:** The aim of this study was to evaluate the role of dual isotope
3 ¹²³Iodine/^{99m}Tc-MIBI thyroid scintigraphy (IMS) in discriminating between malignant and
4 benign suspect nodules using quantitative analysis methods.

5 **Methods:** 35 consecutive patients with thyroid nodules of indeterminate or non-
6 diagnostic cytology and cold on ¹²³Iodine scintigraphy (10 Bethesda I, 24 Bethesda III-IV,
7 1 in which cytology was impossible) underwent IMS between 2017 and 2019 with uptake
8 quantification at two time points ahead of thyroidectomy: early and late. Images were
9 analyzed by two blinded physicians

10 **Results:** 12 nodules were malignant and 23 benign on histopathology. Mean uptake
11 values were lower in benign than in malignant nodules at both time points: early, 8.7±4.1
12 versus 12.9±3.5 (p=0.005); and late, 5.3 ± 2.7 versus 7.7±1.1 (p=0.008). Inter-observer
13 reproducibility was excellent. The intraclass correlation coefficient was 0.86 in benign and
14 0.92 in malignant lesions on the early readings and 0.94 and 0.85 respectively on the late
15 readings. The optimal cut-off to exclude malignancy on late reading was 5.9, with
16 sensitivity, specificity, positive predictive value, negative predictive value and accuracy of
17 respectively, 100%, 65.2%, 60%, 100% and 77.1%.

18 **Conclusion:** Despite some study limitations, quantitative analysis of ^{99m}Tc-MIBI thyroid
19 scintigraphy had a good reproducibility, which could help to rule out malignancy in non-
20 diagnostic or indeterminate thyroid nodules and thereby reducing the number of patients
21 undergoing unnecessary surgery when late uptake is below 5.9.

22 **Résumé**

23 **Contexte :** L'objectif de cette étude est d'évaluer l'apport de la Scintigraphie au ^{99m}Tc-
24 MIBI combinée à l'Iode 123 (SMI) avec quantification de fixation, dans la discrimination
25 bénin-malin des nodules thyroïdiens (NT) suspects.

26 **Patients et méthodes :** 35 patients consécutifs, porteurs d'un NT posant un problème
27 diagnostique de malignité (10 NT Bethesda I, 24 NT Bethesda III-IV, 1 NT d'étude
28 cytologique impossible) ont effectué une SMI avec mesure de la captation du traceur à
29 deux temps d'acquisition précoce (TP) et tardif (TT) avant thyroïdectomie entre 2017 et
30 2019. L'analyse des images de SMI a été réalisée en aveugle par deux praticiens.

31 **Résultats :** 12 nodules étaient malins et 23 bénins en analyse histologique. La moyenne
32 (écart-type) de la mesure de captation du ^{99m}Tc-MIBI était plus élevée dans les cancers
33 au TP (12,9 ± 3,5 vs. 8,7 ± 4,1 ; p=0,005) comme au TT (7,7 ± 1,1 vs. 5,3 ±
34 2,7 ; p=0,008). La reproductibilité inter-observateurs était parfaite. Le coefficient de
35 corrélation intra-classe était de 0,86 (lésions bénignes) et 0,92 (lésions malignes) pour le
36 TP, et de 0,94 (lésions bénignes) et 0,85 (lésions malignes) pour le TT. Le seuil optimal
37 de mesure de captation au TT pour l'exclusion de malignité a été fixé à 5,9. La
38 sensibilité, spécificité, valeur prédictive positive, valeur prédictive négative, et précision
39 de ce seuil étaient respectivement de 100%, 65,2%, 60%, 100% et 77,1% pour
40 différencier un NT bénin et malin.

41 **Conclusion :** Malgré certaines limites, l'analyse quantitative de la scintigraphie
42 thyroïdienne au ^{99m}Tc-MIBI est reproductible et pourrait contribuer à exclure la malignité
43 des nodules thyroïdiens suspects, réduisant ainsi le nombre de thyroïdectomies inutiles
44 lorsque la mesure de captation au TT est inférieure à 5,9.

45 **Keywords:** thyroid nodule, indeterminate or non-diagnostic cytology, ^{99m}Tc-MIBI
46 scintigraphy, malignancy, surgery

47 **Mots clés :** nodule thyroïdien, cytologies indéterminées ou non diagnostiquées,
48 scintigraphie au ^{99m}Tc-MIBI, malignité, chirurgie

53

54

55 **Background**

56 Thyroid nodules are a common clinical problem. Epidemiologic studies have shown that the
57 prevalence of palpable thyroid nodules is approximately 5% in women and 1% in men living in
58 iodine-sufficient parts of the world [1].

59 Both European and American guidelines suggest fine-needle aspiration cytology (FNAC) in
60 combination with ultrasonography (US) for the evaluation of malignancy in thyroid nodules [2–
61 4]. Published data suggest that FNAC has a sensitivity ranging from 65% to 98%, a specificity from
62 72% to 100%, and an overall accuracy of 75% to 90%. Nevertheless, like any other test, FNAC has
63 its limitations and diagnostic traps [5]. In 2–16% of cases, cytology is non-diagnostic and is
64 classified Bethesda category I, i.e., with insufficient material for diagnosis. Moreover, in 5–20% of
65 cases, it is not possible to discriminate between benign and malignant nodules because of an
66 undetermined cytology, including atypia of undetermined significance/follicular lesion of
67 undetermined significance, i.e., Bethesda category III, or because of follicular
68 neoplasm/suspicious for follicular neoplasm, i.e., Bethesda category IV. The risk of malignancy
69 varies from 5% to 10% for non-diagnostic cytology and from 6% to 40% for indeterminate
70 cytology based on the 2017 revision of the Bethesda System for Reporting Thyroid Cytopathology
71 [6]. About 60–95% of patients who underwent thyroidectomy because of non-diagnostic
72 cytology or indeterminate cytology turned out to have a benign lesion at histological evaluation
73 [7,8]. Hence, the use of a non-invasive approach is necessary.

74 In the last two decades, other methods such as molecular testing, nuclear medicine scans,
75 either alone or in combination (i.e. ¹³¹Iodine or ¹²³Iodine or Technetium-99m-
76 methoxyisobutylisonitrile [^{99m}Tc-MIBI] scans combined with either ²⁰¹Thallium or ^{99m}Tc-
77 methoxyisobutylisonitrile or ^{99m}Tc-tetrofosmin), have been used for that purpose.

78 ^{99m}Tc-MIBI is a lipophilic cation that enters the cytoplasm via thermodynamic driving forces and
79 penetrates the mitochondria using the electrical gradient generated by a high negative inner
80 transmembrane mitochondrial potential. The mechanism of cellular ^{99m}Tc-MIBI accumulation has
81 been reported to depend on the size of a tumor, cellular proliferation, the blood flow within it,
82 and the richness of mitochondria in the tumor cells [9,10].

83 ^{99m}Tc-MIBI has been increasingly used to investigate thyroid nodules in order to differentiate
84 between benign and malignant nodules. However, to assess ^{99m}Tc-MIBI retention within the
85 nodules, a majority of authors chose a visual analysis method [11–13]. Two recent meta-analyses
86 with more than 20 studies and including nearly 2000 patients drew similar statements [12,13].
87 They concluded that ^{99m}Tc-MIBI scintigraphy has good sensitivity (85.1 to 87%) but inconstancy
88 and often poor specificity (45.7 to 78%) for predicting the histological malignancy of thyroid
89 nodules. However, as reported in some prospective studies [14,15], adding a quantitative
90 analysis to assess the tracer kinetic by calculating the retention or washout index may increase
91 diagnostic accuracy.

92 In many published studies, ^{99m}Tc-MIBI scintigraphy was combined with ^{99m}Tc-pertechnetate,
93 whereas ¹²³Iodine is more sensitive and allows better selection of cold thyroid nodules in
94 comparison with ^{99m}Tc-pertechnetate [16].

95 The aim of this study was to evaluate the diagnostic performance of dual isotope
96 ¹²³Iodine/^{99m}Tc-MIBI scintigraphy using quantitative analysis in discriminating malignant from
97 benign nodules with indeterminate or non-diagnostic cytology, while verifying the inter-observer
98 reproducibility of the technique.

99

100 **Patients and methods**

101 **a) Study design**

102 A retrospective study was conducted at Lille University Hospital, which recruited patients who
103 had undergone exploration of a thyroid nodule that presented diagnostic difficulty. In cases of
104 difficult diagnosis, patients were offered to undergo a dual isotope ^{123}I odine/ $^{99\text{m}}\text{Tc}$ -MIBI
105 scintigraphy. All patients gave their written informed consent before this procedure. Such cases
106 were discussed in dedicated multidisciplinary meetings. The best treatment option was chosen
107 by the medical and surgical team based on the available guidelines [17] including age, nodule
108 size and progression and the patient's final decision.

109 Only patients who had been operated were analyzed in this study; they were divided into two
110 groups, benign or malignant thyroid nodules, according to the results of the final pathological
111 analysis after surgery, to assess the performance of dual isotope ^{123}I odine/ $^{99\text{m}}\text{Tc}$ -MIBI thyroid
112 scintigraphy in discriminating malignant from benign nodules using quantitative analysis.

113 This study followed the tenants of the Declaration of Helsinki and was approved by the Ethics
114 Committee (N°: DEC19-549) of the Lille University Hospital.

115 **b) Patients**

116 From May 2017 to December 2019, 71 patients were referred from the Endocrinology and
117 Metabolism Department to the Nuclear Medicine Department for thyroid nodule diagnosis with
118 dual isotope ^{123}I odine/ $^{99\text{m}}\text{Tc}$ -MIBI scintigraphy (Figure 1).

119 **b.1) Inclusion and exclusion criteria**

120 **Inclusion criteria**

121 **A.** TSH levels: 0.4 - 4 mU/L.

122 **B.** Nodule > 10 mm in the largest diameter for a multinodular goiter, predominantly solid on
123 US.

124 **C.** A cytological diagnosis of class I, III or IV according to the Bethesda classification system; or
125 FNAC impossible due to the position of the nodule.

126

127 **Exclusion criteria**

128 **A.** Indifferent and hot nodules at ^{123}I evaluation on dual isotope scintigraphy.

129 **B.** Non-operated patients.

130 **c) Study outcomes**

131 All patients underwent physical examination, biological thyroid assays (TSH, FT4, FT3),
132 thyroid US, FNAC (except one patient with an inaccessible nodule) and dual isotope
133 ^{123}I iodine/ $^{99\text{m}}\text{Tc}$ -MIBI scintigraphy.

134 **c.2.1) Ultrasonography**

135 Ultrasound imaging of the thyroid gland and neck region was performed with a high
136 frequency linear ultrasound transducer (ATOSHIBA/Aplio XG™ SSA790A). Thyroid nodules were
137 assessed according to the European Thyroid Imaging Reporting and Data System (EU-TIRADS)
138 classification (EU-TIRADS 1: normal, EU-TIRADS 2: benign, EU-TIRADS 3: low risk of malignancy,
139 EU-TIRADS 4: intermediate risk of malignancy, EU-TIRADS 5: high risk of malignancy) [18].

140 **c.2.2) Fine-needle aspiration cytology**

141 Fine-needle aspiration cytology was indicated according to the criteria recommended by the
142 European and French Societies of Endocrinology [2,4]. FNAC was performed with US guidance.
143 Cytological results were classified according to the Bethesda system [6].

144 **c.2.3) Dual isotope scintigraphy**

145 Dual isotope scintigraphy was carried out in the same day. The total exam time was two and
146 half hours with a radiation dose of about 7.7 millisieverts (mSv) mSv, equivalent to the dose
147 received during a non-injected computed tomography of the abdomen.

148 Thyroid scintigraphy was carried out using a gamma camera equipped with a low-energy
149 pinhole collimator. Radioiodine (5.5 MBq of ^{123}I) was injected first, and $^{99\text{m}}\text{Tc}$ -MIBI (555 MBq)

150 was injected 90 minutes later. Dual isotope static scans in the anterior projection of the neck
151 were performed 20 minutes (early scan) and 60 minutes (late scan) after ^{99m}Tc-MIBI injection.
152 The acquisition time was set at 600 seconds with a 15% window centered on the 140keV peak
153 and a second 15% window centered on the 163keV peak. The focal length (distance between
154 the collimator and the patient's neck) was constant (6 cm) and checked each time.

155 In ¹²³Iodine scintigraphy, thyroid nodules were assessed as being either 1) hyperfunctioning,
156 i.e., hot (uptake in the nodule is greater than uptake in normal thyroid tissue); 2) indifferent, i.e.,
157 warm (uptake in the nodule is equal to uptake in normal thyroid tissue); or 3) hypofunctioning,
158 i.e., cold (uptake in the nodule is less than uptake in normal thyroid tissue).

159 ^{99m}Tc-MIBI scintigraphy was always interpreted comparatively with ¹²³Iodine scintigraphy to
160 exclude indifferent and hot nodules. Scintigraphies were analyzed by two nuclear medicine
161 physicians (AB & LD) who were blinded for clinical data and results of the cytological analysis.

162

163 **Quantitative analysis**

164 ¹²³Iodine and ^{99m}Tc-MIBI images (early and late) were displayed on the same screen for better
165 precision in drawing the region of interest (ROI). A quantitative analysis was also performed by
166 drawing the ROI around the nodule and then mirroring the ROI outside the thyroid to subtract
167 the background activity (figure 1 in supplementary data). ROIs were created on early images and
168 successively copied on delayed ones.

169 Parameters derived from ROI analysis were the mean ^{99m}Tc-MIBI nodular uptake, pixel
170 nodular number, mean ^{99m}Tc-MIBI background uptake and pixel background number.

171 The mean count in each ROI was determined, and early and late uptake results (ER and LR)
172 were calculated as follows:

173 • **Early uptake result (ER)** = mean nodular ^{99m}Tc-MIBI uptake – mean background ^{99m}Tc-

- 174 MIBI uptake (early scans, 20 minutes after injection)
- 175 • **Late uptake result (LR)** = mean nodular ^{99m}Tc -MIBI uptake – mean background ^{99m}Tc -MIBI
- 176 uptake (late scans, 60 minutes after injection)
- 177 • **The MIBI washout index (WOind)** was calculated as a percentage reduction value of the
- 178 mean ^{99m}Tc -MIBI nodular uptake between early (+ 20 minutes) and late (+ 60 minutes)
- 179 scans. **WOind** = $[(\text{LR}/\text{ER}) \times 100] - 100$.

180

181 **c.2.4) Surgery and pathology**

182 Patients underwent total thyroidectomy on the basis of clinical, ultrasonographic and/or

183 cytological criteria. A final histologic diagnosis was obtained after examination of permanent

184 sections of the surgical specimens and served as the reference standard for establishing either

185 the presence or the absence of thyroid malignant tumors.

186 **d) Statistical analysis**

187 Normality of distribution was assessed using histograms and the Shapiro-Wilk test.

188 Quantitative variables were expressed as means (standard deviation) in the case of a normal

189 distribution; otherwise, the median (interquartile range) was used. Categorical variables were

190 expressed as numbers (percentage). Comparisons between the two groups were made using the

191 Student's t-test for Gaussian continuous variables, the Mann-Whitney U test for non-Gaussian

192 continuous variables and the Chi-squared test (or Fisher's exact test for expected cell

193 frequency < 5) for categorical variables, as appropriate.

194 Receiver operating characteristic (ROC) analysis was also performed to determine the LR

195 threshold below which malignant thyroid nodules could be ruled out. The area under the curve

196 (AUC) was calculated to assess the overall accuracy of ^{99m}Tc -MIBI scintigraphy quantitative

197 analysis.

198 We used the intraclass correlation coefficient (ICC) to assess inter-observer reproducibility of
199 quantitative analysis; the ICC is rated good between 0.75 to 0.90 and excellent for values greater
200 than 0.90.

201 Statistical analyses were performed using Graphpad-Prism 7.0 a software, and for ICC
202 analysis, SPSS Version 23 (IBM SPSS Inc., Chicago, IL, USA) using a two-way-random-model. A
203 two-sided p-value of <0.05 was considered statistically significant.

204

205 **Results**

206 The study design flow chart is presented in Figure 1. Seventy-one patients underwent a dual
207 isotope scintigraphy. Of these patients, 5 were excluded because of the presence of a hot
208 nodule, 16 because of indifferent nodules at ¹²³iodine scintigraphy, and 15 because no surgery
209 was performed; therefore 35 patients were included in our study. Demographic,
210 ultrasonographic, cytologic, scintigraphic and pathological data of the 35 patients were
211 summarized in tables 1 and 2 in supplementary data.

212

213 **a) Ultrasound**

214 Most of the thyroid nodules were classified as EU-TIRADS 4 (n=18; 51.4%), ten (28.5%) were
215 EU-TIRADS 3, and seven (20%) were EU-TIRADS 5 (Table 1).

216

217 **b) Fine-needle aspiration cytology**

218 FNAC was available for 34 (96.5%) patients, since one patient had an inaccessible nodule. The
219 cytology results of 19 (55.8%) nodules were classified as Bethesda category IV, 5 (14.7%) were
220 Bethesda III, and 10 (29.4%) were Bethesda I (Table 1).

221

222 **c) Final histological diagnosis**

223 The final histological diagnoses of the thyroidectomy specimens (our reference/gold standard)
224 were 23 (65.7%) benign nodules and 12 (34.2%) malignant nodules (Table 2).

225 The malignant nodules were predominantly papillary thyroid carcinomas (n=6; 50%) and
226 follicular variants of papillary thyroid carcinomas (n=3; 25%). Among the remaining malignant
227 nodules, two were a Hürthle cell carcinomas and one was follicular thyroid carcinoma.

228 Of the 23 patients with benign nodules, 10 had colloid nodular goiters, 10 follicular adenomas,
229 and 3 Hürthle cell adenomas.

230 **d) Comparison between benign and malignant thyroid nodule groups**

231 The mean age at nodule discovery was higher in the benign than in the malignant lesion group
232 (mean age in years \pm SD, respectively, 51.6 ± 14.1 and 38.9 ± 15.7 ; $p= 0.02$). The mean TSH was
233 not significantly different between the malignant and the benign nodule groups (mean of TSH in
234 μ U/mL \pm SD, respectively, 1.01 ± 0.31 and 1.29 ± 0.50 ; $p=0.05$) (Table 1).

235

236 **d.1) Ultrasound**

237 The mean largest diameter of the thyroid nodules was not different between the benign and
238 malignant lesions (32 ± 13.2 mm and 38.5 ± 12.9 mm, respectively; $p = 0.16$). The majority of
239 malignant (8/12; 66.6%) and benign (10/23; 43.4%) nodules were classified EU-TIRADS 4.

240

241 **d.2) Fine-needle aspiration cytology**

242 The prevalence of malignancy was 42.1% (8/19) in nodules with a Bethesda category IV
243 cytology, 20% (1/5) in nodules with a Bethesda category III cytology and 27.3 % (3/11) in a
244 Bethesda category I cytology.

245 Most nodules with malignant histology had a Bethesda category IV cytology result (n=8; 66.6%),
246 25% (3/12) were Bethesda I and one nodule was Bethesda III. Of the 23 nodules with benign
247 histology, 11 (50%) had a Bethesda category IV cytology result, 4 (18.2%) were Bethesda III, and 7
248 (31.8%) were Bethesda I. FNAC had not been performed in one patient because of an
249 inaccessible nodule.

250

251 **d.3) Quantitative analysis of ^{99m}Tc-MIBI scintigraphy**

252 Quantitative analysis of ^{99m}Tc-MIBI scintigraphy data showed that early (ER) and late (LR)
253 ^{99m}Tc-MIBI uptake results were significantly higher in malignant than in benign nodules for both
254 physicians (Table 3, Figures 2A and B). The difference was highly significant for the two nuclear
255 medicine physicians concerning ER in malignant versus benign lesions. The difference was also
256 highly significant in LR between malignant and benign thyroid nodules. We found the same
257 results when comparing the means of ER and LR measurements of both physicians.

258 Inter-observer reproducibility between the two physicians was assessed by ICC. The ICC of ER
259 was 0.86 (95% CI: [0.58-0.94]; p=0.0001) for benign nodules, and 0.92 (95% CI: [0.72-0.97];
260 p=0.0001) for malignant lesions. For LR, the ICC was 0.94 (95% CI: [0.85-0.97]; p=0.0001) for
261 benign nodules and 0.85 (95% CI: [0.48-0.95] for malignant nodules (Figure 3).

262 There was no difference in the wash-out index between malignant and benign nodules (Table
263 3).

264 Using ROC curve analysis, the optimal cut-off for ER and LR corresponding to the highest
265 accuracy for discriminating between benign and malignant thyroid lesions was set at 6.6 and 5.9,
266 respectively. The AUC for ER was 0.78 (95% CI = 0.62 to 0.93; p= 0.006), and it was 0.78 (95% CI =
267 0.63 to 0.94; p= 0.005) for LR (Figures 2 D & E). Accordingly, 26 nodules had an ER greater than
268 6.6, of which 12 were histologically malignant and 14 had a benign histology. The remaining 9
269 nodules with an ER equal to or below this cut-off were all histologically benign. The sensitivity

270 and specificity of ^{99m}Tc-MIBI quantitative analysis for this cut-off were 100% and 39.1%,
271 respectively. Positive predictive value, negative predictive value and accuracy were 46.1%, 100%
272 and 60%, respectively.

273 Of the 20 nodules with an LR over 5.9, 12 had a malignant histology, whereas 8 were
274 histologically benign (5 follicular adenomas, 2 Hürthle cell adenomas and one colloid nodular
275 goiter). The remaining 15 nodules with an LR equal to or below this cut-off were all histologically
276 benign (11 colloid nodular goiters, 4 follicular adenomas and one Hürthle cell adenoma). The
277 sensitivity and specificity of ^{99m}Tc-MIBI quantitative analysis for this cut-off were 100% and
278 65.2%, respectively. Positive and negative predictive values and accuracy were 60%, 100% and
279 77.1%, respectively.

280 Therefore, LR had higher accuracy as well as a higher specificity and positive predictive value
281 than ER for discriminating between benign and malignant thyroid lesions.

282 **Discussion**

283 In our series, the use of dual isotope ¹²³iodine/^{99m}Tc-MIBI scintigraphy allowed to exclude
284 malignancy in euthyroid nodules with indeterminate or non-diagnostic cytology in a two steps
285 evaluation. First, hot and warm nodules at ¹²³iodine evaluation were excluded since the ¹²³iodine
286 uptake orientates in practice toward the benignity. Secondly, we used quantitative analysis of
287 ^{99m}Tc-MIBI scintigraphy to further characterize cold nodules, since only 16% of them are
288 reported to be malignant [19]. We thus found that the means of ^{99m}Tc-MIBI ER and LR were
289 higher in malignant than in benign nodules. Moreover, LR had higher accuracy as well as a higher
290 specificity and positive predictive value than ER for discriminating between benign and malignant
291 thyroid lesions. Accordingly, using ROC curve the optimal LR cut-off that differentiated malignant
292 from benign lesions was set at 5.9, with a sensitivity, specificity, positive predictive value,
293 negative predictive value and accuracy of 100%, 65.2%, 60%, 100% and 77.1%, respectively. This

294 means that when the LR is < 5.9, benignity is certain. When the LR is >5.9, the risk of malignancy
295 reaches 60%, and surgical thyroidectomy should be considered.

296 To our knowledge, this is the first report to describe the usefulness of LR measurement in the
297 quantitative analysis of ^{99m}Tc-MIBI scintigraphy for ruling out malignancy of thyroid nodules with
298 excellent sensitivity. Only two previous studies reported the usefulness of LR in quantitative
299 analysis of ^{99m}Tc-MIBI scintigraphy to discriminate between malignant and benign nodules, but
300 with a sensitivity of 61% and 83.3%, respectively [20,21].

301 In our study, all malignant nodules were correctly detected, but eight benign nodules were
302 falsely positive (40%), of which six were follicular adenomas and two were Hürthle cell
303 adenomas. All thyroid nodules with LR equal to or below this cut-off were histologically benign
304 (10 colloid nodular goiter, 4 follicular adenomas and one Hürthle cell adenoma). Contrary to
305 follicular adenomas, there was no colloid nodular goiter with an LR over the cut-off of 5.9,
306 probably because the cell abundance is greater in follicular adenomas than in colloid nodular
307 goiters. Similar results were reported by other authors [22].

308 Indeed, ¹²³Iodine/^{99m}Tc-MIBI scintigraphy with additional quantitative analysis seems to be an
309 accurate method for evaluation of thyroid nodules with indeterminate or non-diagnostic
310 cytology.

311 Moreover, in addition to the already known data, we report for the first time a very good
312 inter-observer reproducibility for the quantitative analysis of ^{99m}Tc-MIBI scintigraphy for both ER
313 and LR in malignant and benign nodules.

314 Various methods of quantitative ^{99m}Tc-MIBI analysis have been proposed through many
315 studies [15,23,24]. Recently, the implementation of the wash-out index was found to be more
316 accurate than the retention index in discriminating malignant from benign cytological
317 indeterminate thyroid nodules, with an overall accuracy of 100% versus 62.5%, respectively [25].

318 In contrast with our study, given that the kinetic decrease in ^{99m}Tc -MIBI uptake (at 60 minutes)
319 was similar in both malignant and benign lesions, there was no difference in the wash-out index
320 between the two groups ($p=0.94$), and ^{99m}Tc -MIBI uptake in malignant lesions remained greater
321 than in benign lesions. Hence, the use of the ^{99m}Tc -MIBI washout index in our study was not
322 useful for differentiating benign from malignant thyroid nodules, as previously reported in
323 another study including 43 patients with a solitary cold thyroid nodule, 9 of which were
324 malignant and 34 benign [26].

325 The disparity between the results of previous studies can be explained, on the one hand, by
326 the difference between protocols that were used, including the image acquisition times, and, on
327 the other hand, by the fact that quantitative analysis is at least partially an instrument-
328 dependent technique [27]. For these reasons, it is important to acknowledge that our results are
329 specific to our center and that each department of nuclear medicine needs to set its own LR cut-
330 off. Multicenter studies with a standard protocol are needed before being able to generalize and
331 integrate ^{99m}Tc -MIBI scintigraphy in the guidelines of thyroid nodule evaluation.

332 Among several radioisotope imaging techniques, some recent studies have explored the role
333 of Fluorine-18-fluorodeoxyglucose (^{18}F -FDG) positron emission tomography (PET)-computed
334 tomography (CT) in discriminating benign from malignant thyroid nodules [28]. It was reported
335 that ^{18}F -FDG PET/CT had a higher diagnostic performance in discriminating between benign and
336 malignant indeterminate thyroid nodules compared to visual analysis of ^{99m}Tc -MIBI scintigraphy
337 [29]. However, quantitative analysis of ^{99m}Tc -MIBI scintigraphy is more accurate than the visual
338 analysis approach [25]. Also, a recent meta-analysis of eight studies reported that ^{18}F -FDG
339 PET/CT had a moderate ability to correctly discriminate malignant from benign lesions [28].

340 Despite our encouraging results, some other limitations should be acknowledged. One of the
341 limitations of ^{99m}Tc -MIBI scintigraphy is the impossibility of discriminating between Hürthle cell
342 adenomas and Hürthle cell carcinomas, which has already been reported by several authors

343 [15,25,26,30–32]. The high uptake of ^{99m}Tc -MIBI by Hürthle cells is likely related to the negative
344 transmembrane mitochondrial electric potential [9,33].

345 Also, in our study only patients who had undergone surgery and had definitive histology of the
346 indeterminate cold thyroid nodule were included. Ideally, histological classification of all nodules,
347 from the initial cohort of 50 patients with a cold nodule, should be available to evaluate the
348 validity of a diagnostic approach. However, the majority of non-operated cold nodules remained
349 stable on US monitoring. Of these nodules, only one had an LR over the cut-off of 5.9, and
350 surgery was delayed due to other health issues.

351 The low number of patients in our study cohort could also be a limiting factor. Nevertheless,
352 similar results were reported by the same team in two series of 20 and 105 patients,
353 respectively, using quantitative analysis of ^{99m}Tc -MIBI [22,25].

354 To sum up, in euthyroid patients, quantitative analysis of ^{99m}Tc -MIBI scintigraphy could be
355 proposed as a second-line procedure for predicting malignant risk of solid thyroid nodules > 1cm,
356 with indeterminate or non-diagnostic cytology and cold at ^{123}I iodine scintigraphy.

357 Nodules with LR uptake below or equal to the cut-off of 5.9, in which malignancy can be
358 excluded, support clinical and US follow-up. On the contrary, surgical treatment should be
359 discussed for thyroid nodules with LR uptake over the cut-off of 5.9 because of their high risk of
360 malignancy, reaching 60% in our study.

361

362 In conclusion, despite some limitations, our results suggest that dual isotope ^{123}I iodine/ ^{99m}Tc -
363 MIBI scintigraphy is an effective adjunctive pre-surgical method with a good interobserver
364 reproducibility, in combination with both US and FNAC, for ruling out malignancy of thyroid
365 nodules, thus reducing the number of unnecessary thyroidectomies. However, further
366 multicenter trial in larger series of patients will be necessary before being able to generalize and

367 integrate quantitative analysis of ^{99m}Tc-MIBI scintigraphy in the guidelines of thyroid nodules
368 management.

369

370

371 **Availability of data and materials:** All data generated or analysed during this study are included
372 in this published article (and its supplementary information files).

373 **Acknowledgments:** The authors would like to thank endocrinologists from the Nord and Pas-de-
374 Calais departments who participated in patient recruitment for the study. The authors also thank
375 Janet Ratiu for the English review of the manuscript.

376 **Declaration of interest:** The authors declare that there is no conflict of interest that could be
377 perceived as prejudicing the impartiality of the research reported.

378 **Funding:** This research did not receive any specific grant from any funding agency in the public,
379 commercial or nonprofit sector.

380

381

382

383

384

385

386

387

388

389

390

391

392

393

394

395 **References:**

396 [1] Dean DS, Gharib H. Epidemiology of thyroid nodules. *Best Pract Res Clin Endocrinol*
397 *Metab* 2008;22:901–11. <https://doi.org/10.1016/j.beem.2008.09.019>.

398 [2] Leenhardt L, Borson-Chazot F, Calzada M, Carnaille B, Charrié A, Cochand-Priollet B, et al.
399 Good practice guide for cervical ultrasound scan and echo-guided techniques in treating
400 differentiated thyroid cancer of vesicular origin. *Ann Endocrinol* 2011;72:173–97.
401 <https://doi.org/10.1016/j.ando.2011.04.001>.

402 [3] Haugen BR, Alexander EK, Bible KC, Doherty GM, Mandel SJ, Nikiforov YE, et al. 2015
403 American Thyroid Association Management Guidelines for Adult Patients with Thyroid Nodules
404 and Differentiated Thyroid Cancer: The American Thyroid Association Guidelines Task Force on
405 Thyroid Nodules and Differentiated Thyroid Cancer. *Thyroid* 2016;26:1–133.
406 <https://doi.org/10.1089/thy.2015.0020>.

407 [4] Paschke R, Cantara S, Crescenzi A, Jarzab B, Musholt TJ, Sobrinho Simoes M. European
408 Thyroid Association Guidelines regarding Thyroid Nodule Molecular Fine-Needle Aspiration
409 Cytology Diagnostics. *Eur Thyroid J* 2017;6:115–29. <https://doi.org/10.1159/000468519>.

410 [5] Singh Ospina N, Iñiguez-Ariza NM, Castro MR. Thyroid nodules: diagnostic evaluation
411 based on thyroid cancer risk assessment. *BMJ* 2020;l6670. <https://doi.org/10.1136/bmj.l6670>.

412 [6] Cibas ES, Ali SZ. The 2017 Bethesda System for Reporting Thyroid Cytopathology. *Thyroid*
413 2017;27:1341–6. <https://doi.org/10.1089/thy.2017.0500>.

414 [7] Wang C-CC, Friedman L, Kennedy GC, Wang H, Kebebew E, Steward DL, et al. A Large
415 Multicenter Correlation Study of Thyroid Nodule Cytopathology and Histopathology. *Thyroid*
416 2011;21:243–51. <https://doi.org/10.1089/thy.2010.0243>.

417 [8] Bongiovanni M, Bellevisine C, Troncone G, Sykiotis GP. Approach to cytological
418 indeterminate thyroid nodules. *Gland Surg* 2019;8:S98–104.
419 <https://doi.org/10.21037/gs.2018.12.06>.

420 [9] Moretti J-L, Hauet N, Caglar M, Rebillard O, Burak Z. To use MIBI or not to use MIBI? That
421 is the question when assessing tumour cells. *Eur J Nucl Med Mol Imaging* 2005;32:836–42.
422 <https://doi.org/10.1007/s00259-005-1840-x>.

423 [10] Sarikaya A, Huseyinova G, Irfano??Lu ME, Erkmén N, Ermik TF, Berkarda S. The
424 relationship between 99Tcm-sestamibi uptake and ultrastructural cell types of thyroid tumours:
425 *Nucl Med Commun* 2001;22:39–44. <https://doi.org/10.1097/00006231-200101000-00006>.

426 [11] Hurtado-López L-M, Martínez-Duncker C. Negative MIBI thyroid scans exclude
427 differentiated and medullary thyroid cancer in 100% of patients with hypofunctioning thyroid
428 nodules. *Eur J Nucl Med Mol Imaging* 2007;34:1701–3. <https://doi.org/10.1007/s00259-007-0490-6>.

430 [12] Treglia G, Caldarella C, Saggiorato E, Ceriani L, Orlandi F, Salvatori M, et al. Diagnostic
431 performance of 99mTc-MIBI scan in predicting the malignancy of thyroid nodules: a meta-
432 analysis. *Endocrine* 2013;44:70–8. <https://doi.org/10.1007/s12020-013-9932-z>.

433 [13] Kim S-J, Lee S-W, Jeong SY, Pak K, Kim K. Diagnostic Performance of Technetium-99m
434 Methoxy-Isobutyl-Isonitrile for Differentiation of Malignant Thyroid Nodules: A Systematic

435 Review and Meta-Analysis. *Thyroid* 2018;28:1339–48. <https://doi.org/10.1089/thy.2018.0072>.

436 [14] Riazi A, Kalantarhormozi M, Nabipour I, Eghbali SS, Farzaneh M, Javadi H, et al.
437 Technetium-99m methoxyisobutylisonitrile scintigraphy in the assessment of cold thyroid
438 nodules: is it time to change the approach to the management of cold thyroid nodules? *Nucl*
439 *Med Commun* 2014;35:51–7. <https://doi.org/10.1097/MNM.000000000000013>.

440 [15] Saggiorato E, Angusti T, Rosas R, Martinese M, Finessi M, Arecco F, et al. 99mTc-MIBI
441 Imaging in the Presurgical Characterization of Thyroid Follicular Neoplasms: Relationship to
442 Multidrug Resistance Protein Expression. *J Nucl Med* 2009;50:1785–93.

443 [16] Huysmans DA, Hermus AR. Iodine and Technetium Scintigraphy of the Thyroid. In: de
444 Herder WW, editor. *Funct. Morphol. Imaging Endocr. Syst.*, vol. 7, Boston, MA: Springer US;
445 2000, p. 103–24. https://doi.org/10.1007/978-1-4615-4341-1_6.

446 [17] Nabhan F, Ringel MD. Thyroid nodules and cancer management guidelines: comparisons
447 and controversies. *Endocr Relat Cancer* 2017;24:R13–26. <https://doi.org/10.1530/ERC-16-0432>.

448 [18] Russ G, Bonnema SJ, Erdogan MF, Durante C, Ngu R, Leenhardt L. European Thyroid
449 Association Guidelines for Ultrasound Malignancy Risk Stratification of Thyroid Nodules in Adults:
450 The EU-TIRADS. *Eur Thyroid J* 2017;6:225–37. <https://doi.org/10.1159/000478927>.

451 [19] Rager O, Radojewski P, Dumont RA, Treglia G, Giovanella L, Walter MA. Radioisotope
452 imaging for discriminating benign from malignant cytologically indeterminate thyroid nodules.
453 *Gland Surg* 2019;8:S118–25. <https://doi.org/10.21037/gs.2019.03.06>.

454 [20] Erdil TY, Özker K, Kabasakal L, Kanmaz B, Sönmezoglu K, Atasoy KÇ, et al. Correlation of
455 technetium-99m MIBI and thallium-201 retention in solitary cold thyroid nodules with
456 postoperative histopathology. *Eur J Nucl Med Mol Imaging* 2000;27:713–20.
457 <https://doi.org/10.1007/s002590050567>.

458 [21] Rafat AS, Sherin W, Azza S, Ashraf F. Evaluation of Solitary Thyroid Cold Nodules
459 with Technetium-99m Sestamibi and Thallium-201. *J Egypt Natl Cancer Inst* 2001;13:147–55.

460 [22] Campennì A, Siracusa M, Ruggeri RM, Laudicella R, Pignata SA, Baldari S, et al.
461 Differentiating malignant from benign thyroid nodules with indeterminate cytology by 99mTc-
462 MIBI scan: a new quantitative method for improving diagnostic accuracy. *Sci Rep* 2017;7:6147.
463 <https://doi.org/10.1038/s41598-017-06603-3>.

464 [23] Giovanella L, Suriano S, Maffioli M, Ceriani L, Spriano G. ^{99m}Tc-sestamibi scanning in
465 thyroid nodules with nondiagnostic cytology. *Head Neck* 2009:NA-NA.
466 <https://doi.org/10.1002/hed.21229>.

467 [24] Theissen P, Schmidt M, Ivanova T, Dietlein M, Schicha H. MIBI scintigraphy in
468 hypofunctioning thyroid nodules: Can it predict the dignity of the lesion? *Nuklearmedizin*
469 2009;48:144–52. <https://doi.org/10.3413/nukmed-0240>.

470 [25] Campennì A, Giovanella L, Siracusa M, Alibrandi A, Pignata SA, Giovinazzo S, et al. 99mTc-
471 Methoxy-Isobutyl-Isonitrile Scintigraphy Is a Useful Tool for Assessing the Risk of Malignancy in
472 Thyroid Nodules with Indeterminate Fine-Needle Cytology. *Thyroid* 2016;26:1101–9.
473 <https://doi.org/10.1089/thy.2016.0135>.

474 [26] Demirel K, Kapucu Ö, Yücel C, Özdemir H, Ayvaz G, Taneri F. A comparison of radionuclide
475 thyroid angiography, 99mTc-MIBI scintigraphy and power Doppler ultrasonography in the
476 differential diagnosis of solitary cold thyroid nodules. *Eur J Nucl Med Mol Imaging* 2003;30:642–
477 50. <https://doi.org/10.1007/s00259-003-1124-2>.

478 [27] Schenke S, Klett R, Acker P, Rink T, Kreissl MC, Zimny M. Interobserver Agreement of
479 Planar and SPECT Tc99m-MIBI Scintigraphy for the Assessment of Hypofunctioning Thyroid
480 Nodules. *Nuklearmedizin* 2019;58:258–64. <https://doi.org/10.1055/a-0894-4843>.

481 [28] Castellana, Trimboli, Piccardo, Giovanella, Treglia. Performance of 18F-FDG PET/CT in
482 Selecting Thyroid Nodules with Indeterminate Fine-Needle Aspiration Cytology for Surgery. A
483 Systematic Review and a Meta-Analysis. *J Clin Med* 2019;8:1333.

484 <https://doi.org/10.3390/jcm8091333>.

485 [29] Piccardo A, Puntoni M, Treglia G, Foppiani L, Bertagna F, Paparo F, et al. Thyroid nodules
486 with indeterminate cytology: prospective comparison between 18F-FDG-PET/CT, multiparametric
487 neck ultrasonography, 99mTc-MIBI scintigraphy and histology. *Eur J Endocrinol* 2016;174:693–
488 703. <https://doi.org/10.1530/EJE-15-1199>.

489 [30] Vattimo A, Bertelli P, Cintorino M, Burroni L, Volterrani D, Vella A. Identification of
490 Hürthle cell tumor by single-injection, double-phase scintigraphy with technetium-99m-
491 sestamibi. *J Nucl Med Off Publ Soc Nucl Med* 1995;36:778–82.

492 [31] Boi F, Lai M, Deias C, Piga M, Serra A, Uccheddu A, et al. The usefulness of 99mTc-
493 SestaMIBI scan in the diagnostic evaluation of thyroid nodules with oncocyctic cytology. *Eur J*
494 *Endocrinol* 2003:493–8.

495 [32] Chamnanrabiabkij E, Welch A, Jayapaul MK, Perros P. Detection of Hurthle Cell Carcinoma
496 Using Sestamibi. *Thyroid* 2008;18:575–6.

497 [33] Piwnica-Worms D, Kronauge JF, LeFurgey A, Backus M, Hockett D, Ingram P, et al.
498 Mitochondrial localization and characterization of 99Tc-SESTAMIBI in heart cells by electron
499 probe X-ray microanalysis and 99Tc-NMR spectroscopy. *Magn Reson Imaging* 1994;12:641–52.
500 [https://doi.org/10.1016/0730-725X\(94\)92459-7](https://doi.org/10.1016/0730-725X(94)92459-7).

501

502

503

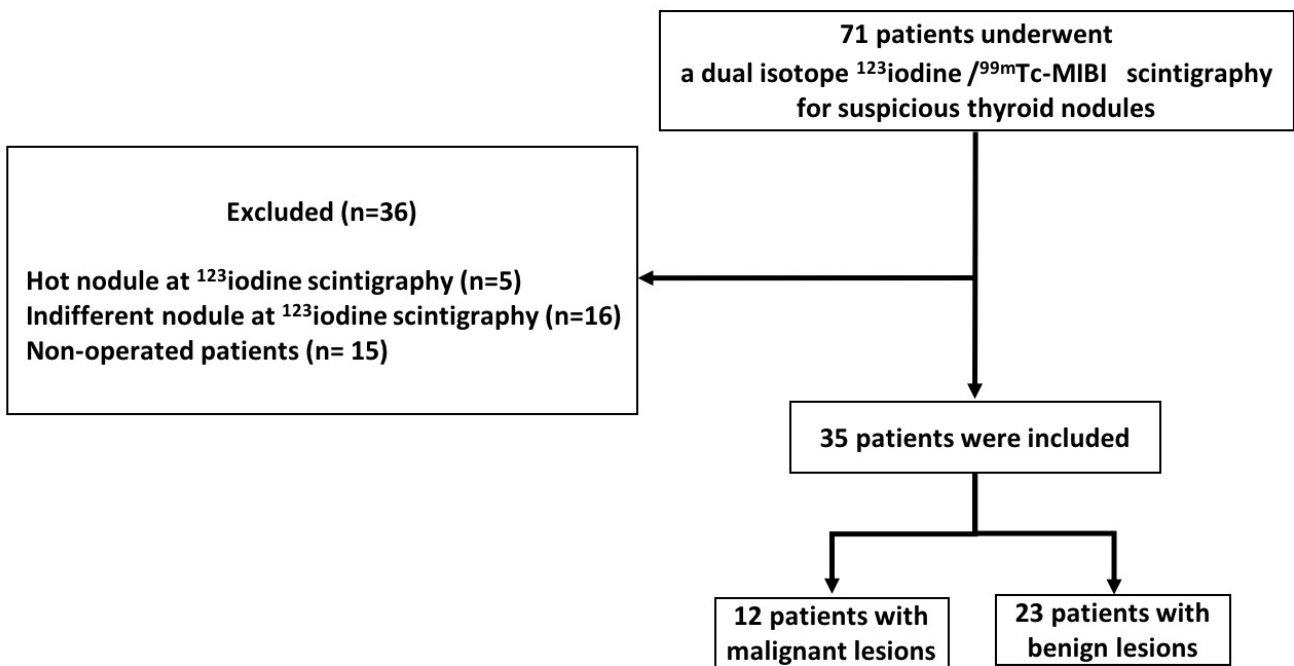


Figure 1. Flow chart of the study. 35 patients were operated and included

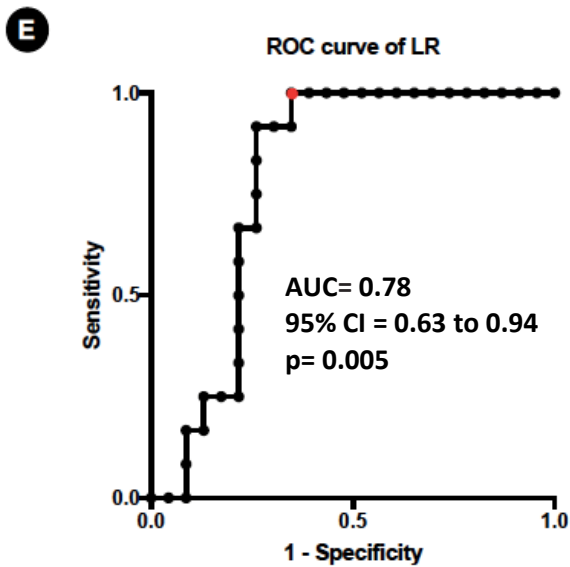
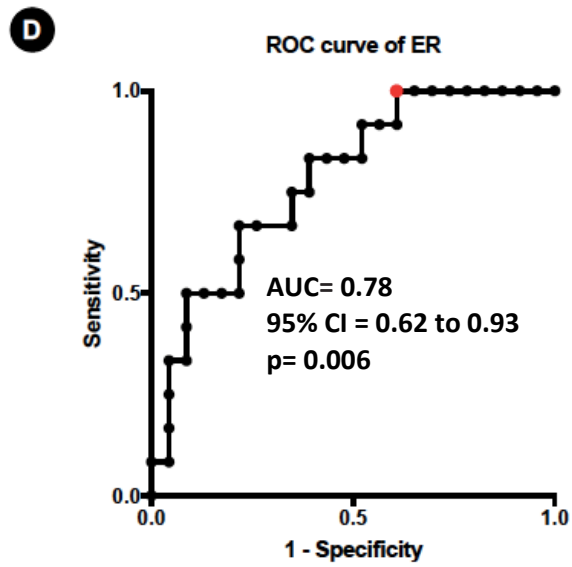
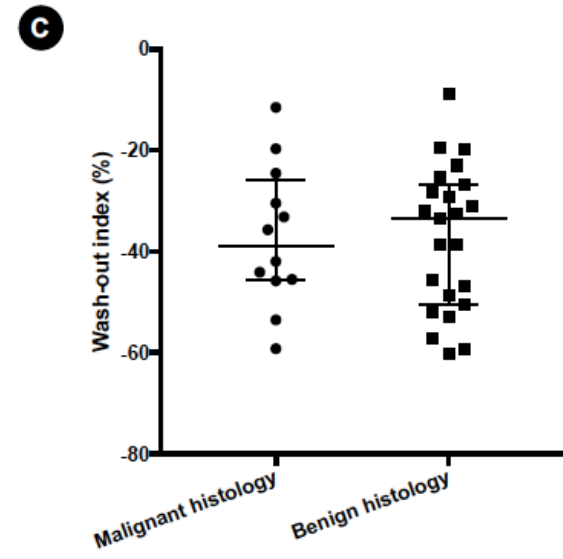
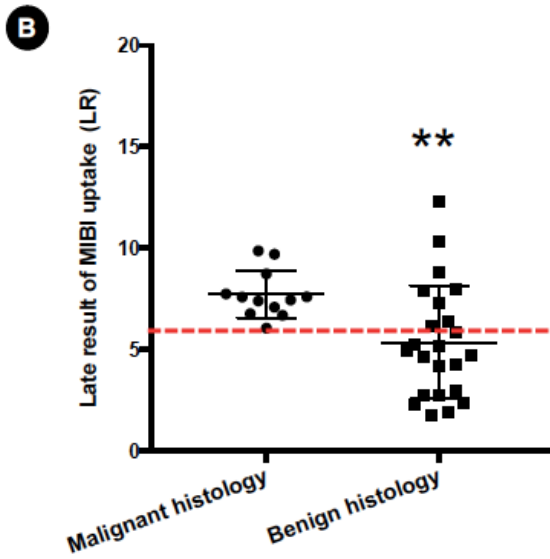
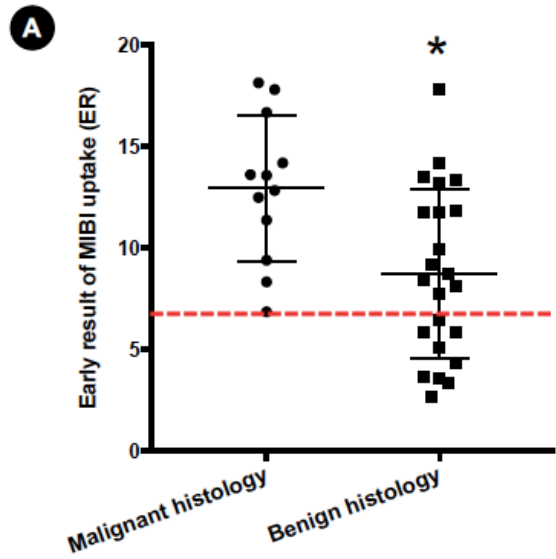


Figure 2. Average measurements of (A) ER, (B) LR, (C) wash-out index in both malignant and benign groups. Dot and square plots depict ER and LR values from the 12 patients with malignant lesions, and the 23 patients with benign lesions, respectively; horizontal bars detail median and interquartile values. Red dashed lines represent the ER (6.6) and LR cut-offs (5.9). *(p= 0.005), **(p=0.008).

(D), (E) Receiver operating characteristic (ROC) analysis of malignant versus benign lesions. Red dots depict optimal cut-off for ER (6.6) and LR (5.9). Area under the ROC curve (AUC) for ER = 0.78; (95% CI = 0.62 to 0.93; p= 0.006), and AUC for LR= 0.78; (95% CI = 0.63 to 0.94; p= 0.005). **For the ER cut-off:** Sensitivity, specificity, positive predictive value (PPV), negative predictive value (NPV) and accuracy: **100%** (95% CI: [75.7-100]), **39.1%** (95% CI: [22.1-59.2]), **46.1%** (95% CI: [28.7-64.5]), **100%** (95% CI: [70-100]) and **60%**, respectively. **For the LR cut-off:** Sensitivity, specificity, positive predictive value (PPV), negative predictive value (NPV) and accuracy: **100%** (95% CI: [75.7-100]), **65.2%** (95% CI: [44.8-81.1]), **60%** (95% CI: [38.6-78.1]), **100%** (95% CI: [79.6-100]) and **77.1%**, respectively.

Abbreviations: AUC: Area Under the Curve, 95% CI: 95% Confidence Interval. ER & LR: Early and late result of ^{99m}Tc-MIBI uptake within nodules, respectively.

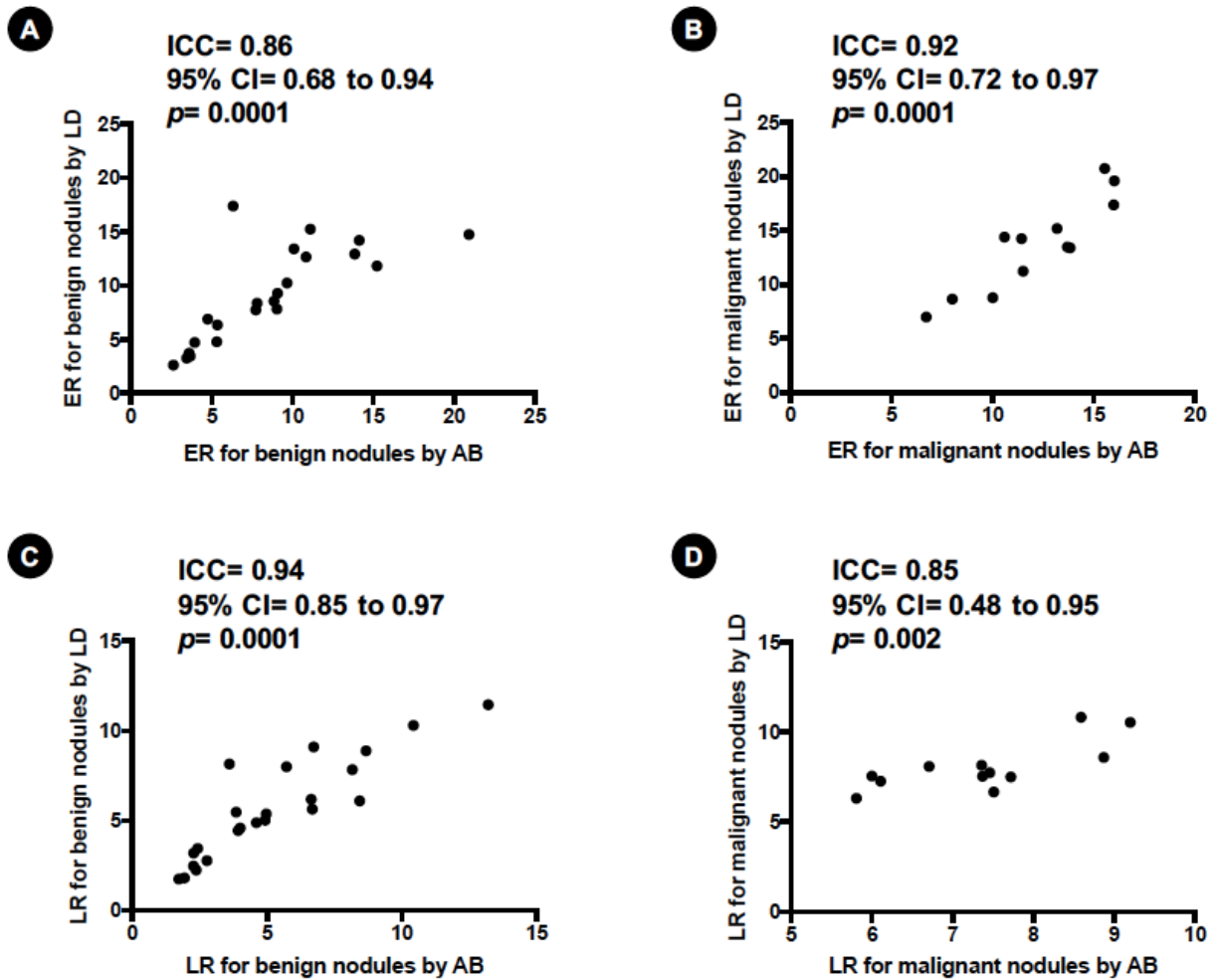


Figure 3. Intraclass correlation coefficients (ICC) between both physicians (AB and LD) of ER for benign (A), malignant lesions (B) and of LR for benign (C), malignant lesions (D).

Abbreviations: 95% CI: 95% Confidence Interval, ER & LR: Early and late result of ^{99m}Tc -MIBI uptake within nodule, respectively.

Table 1. Characteristics of patients (subdivided into those with benign and malignant histological findings after surgery).

Parameters	Malignant (N = 12)	Benign (N = 23)	nodules N = 35	p-value
Age* (mean \pm SD, years)	38.9 \pm 15.7	51.6 \pm 14.1		0.02
Sex ratio	1 : 3	1 : 2.3		0.73
TSH (mean \pm SD; μ IU/mL)	1.29 \pm 0.50	1.01 \pm 0.31		0.05
Duration of follow-up since thyroid nodules discovery (median (IQR), months)	34.5 (25.7; 86.2)	23 (14; 56)		0.06
Duration of follow-up since MIBI scintigraphy (median (IQR), months)	6 (4; 9.2)	6 (5; 10)		0.52
Largest diameter of the nodule (mean \pm SD, mm)	38.5 \pm 12.9	32 \pm 13.2		0.16
US classification				
EU-TIRADS 5 (n, %)	2 (16.6)	5 (21.7)	7 (20)	
EU-TIRADS 4 (n, %)	8 (66.6)	10 (43.4)	18 (51.4)	
EU-TIRADS 3 (n, %)	2 (16.6)	8 (34.7)	10 (28.5)	
FNAC				
Bethesda IV (n, %)	8 (66.6)	11 (50)	19 (55.9)	
Bethesda III (n, %)	1 (8.3)	4 (18.2)	5 (14.7)	
Bethesda I (n, %)	3 (25)	7 (31.8)	10 (29.4)	
Not done	0	1	1	

Abbreviations: IQR Interquartile, SD standard deviation, MIBI ^{99m}Tc -MIBI, US Ultrasound, FNAC Fine needle aspiration cytology.

*Age of the patient when thyroid nodule was discovered.

Table 2. Summary of final histological diagnosis and ^{99m}Tc-MIBI scintigraphy findings.

Histology	(n, %)	^{99m} Tc-MIBI scintigraphy	
		Quantitative analysis n= 35	
		LR cut-off > 5.9	LR cut-off ≤ 5.9
Benign			
Hürthle cell adenoma	3 (13%)	2	1
Follicular adenoma	10 (43.5%)	6	4
Colloid nodular goiter	10 (43.5%)	0	10
Total	23 (100%)	8	15
Malignant			
Hürthle cell carcinoma	2 (16.6%)	2	0
Papillary thyroid carcinoma	6 (50%)	6	0
Follicular variant of papillary thyroid carcinoma	3 (25%)	3	0
Follicular thyroid carcinoma	1 (8.3%)	1	0
Total	12 (100%)	12	0

Abbreviations: ER & LR: Early and late result of ^{99m}Tc-MIBI uptake within nodules, respectively.

Table 3. Summary of quantitative methods for ^{99m}Tc-MIBI scintigraphy findings.

	Malignant	Benign	P-value
	N = 12	N = 23	
Parameters			
MIBI scintigraphy analysis by AB			
ER (Mean ± SD (median, IQR))	12.2 ± 3 12.3 (10.1; 15.1)	8.4 ± 4.5 7.8 (4.7; 10.8)	0.01
LR (Mean ± SD (median, IQR))	7.4 ± 1.1 7.4 (6.2; 8.3)	5.2 ± 3 4.6 (2.4; 6.7)	0.007
Wash-out index (Mean ± SD (median, IQR))	-36 ± 12.4 -35.3 (-45.6; -25.3)	-37.3 ± 13.2 -38 (-46.3; -26.1)	0.77
MIBI scintigraphy analysis by LD			
ER (Mean ± SD (median, IQR))	13.6 ± 4.2 13.8 (9.4; 16.8)	8.9 ± 4.3 8.3 (4.7; 12.9)	0.004
LR (Mean ± SD (median, IQR))	8 ± 1.3 7.6 (7.3; 8.4)	5.4 ± 2.7 5 (3.2; 7.8)	0.004
Wash-out index (Mean ± SD (median, IQR))	-37.1 ± 15.3 40.1 (-47.4; -25.7)	-36.6 ± 16.1 -32.8 (-50.9; -27.4)	0.94
MIBI scintigraphy analysis (average: AB & LD)			
ER (Mean ± SD (median, IQR))	12.9 ± 3.5 13.2 (9.8; 16)	8.7 ± 4.1 8.4 (5; 11.8)	0.005
LR (Mean ± SD (median, IQR))	7.7 ± 1.1 7.5 (6.8; 8.4)	5.3 ± 2.7 4.9 (2.7; 7.2)	0.008
Wash-out index (Mean ± SD (median, IQR))	-37 ± 13.9 (-38.8) (-45.7; -26)	-37.4 ± 14.2 -33.5 (-50.4; -26.8)	0.95

Abbreviations: SD Standard deviation, IQR Interquartile, MIBI ^{99m}Tc-MIBI, ER & LR : Early and late result of ^{99m}Tc-MIBI uptake within nodules, respectively.